Supporting Information

Flexible, Optically Transparent, High Refractive, and Thermally Stable Polyimide/TiO_2 Hybirds for Anti-Reflection Coating

By *Hung-Ju Yen,*[T] *Chia-Liang Tsai,*[T] *Pei-Hsuan Wang, Jiang-Jen Lin,* and *Guey-Sheng Liou**

Functional Polymeric Materials Laboratory, Institute of Polymer Science and Engineering,

National Taiwan University, Taipei, Taiwan

Tel: +886-2-336-5315; Fax: +886-2-336-5237; E-mail: gsliou@ntu.edu.tw

T equal contribution to this work

List of Contents for Supplementary Material:

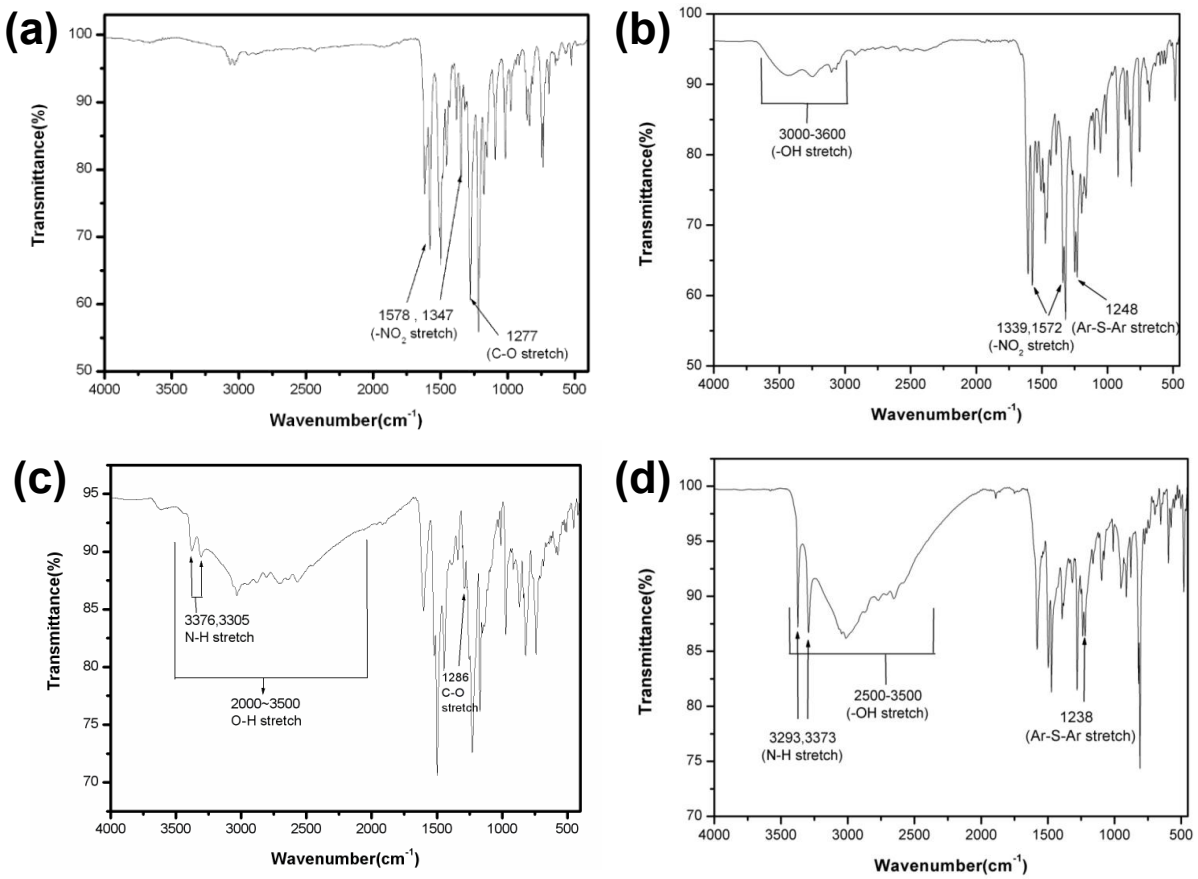

Figure S1. FTIR spectra of compounds (a) **F-DN**, (b) **3S-DN**, (c) **F-DN**, and (d) **3S-DN**.

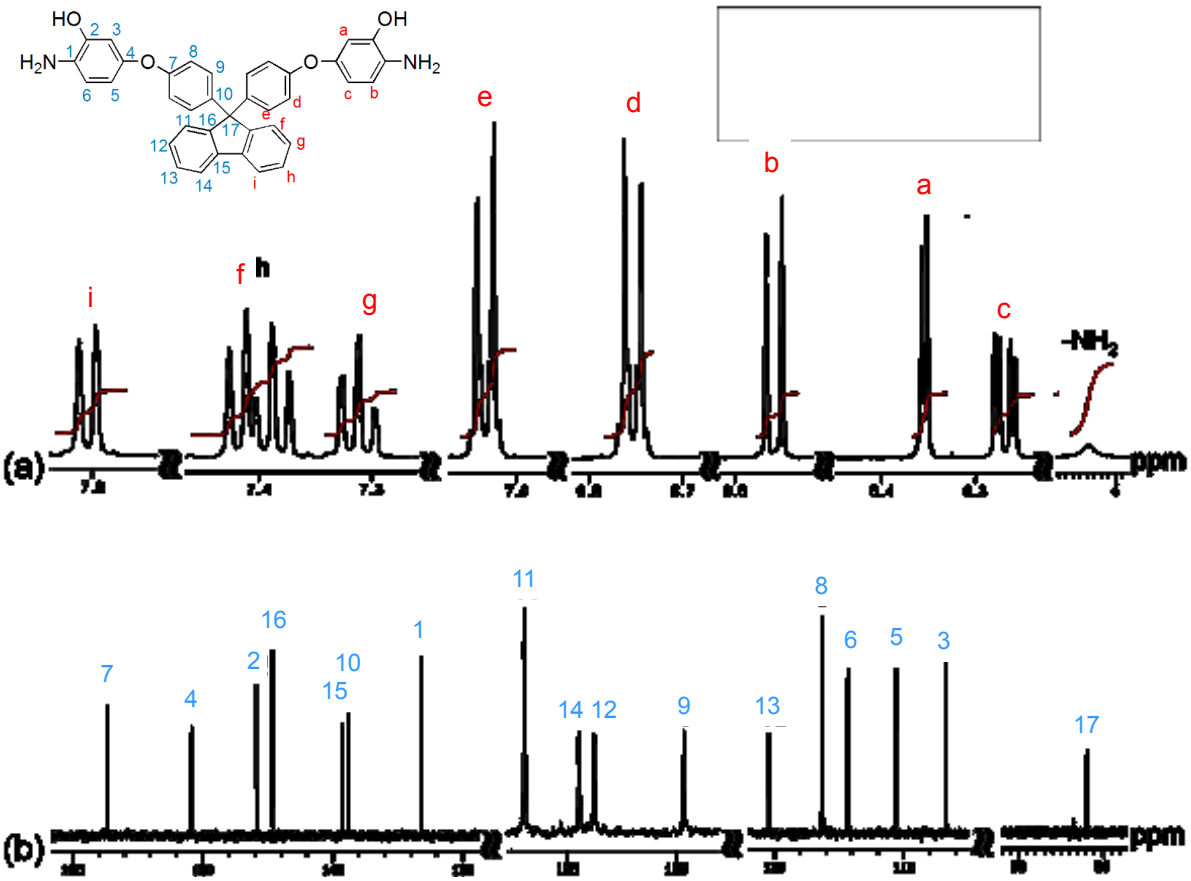

Figure S2. (a) ^{1}H NMR and **(b)** ^{13}C NMR spectra of compound **F-DA** in DMSO-d_6.

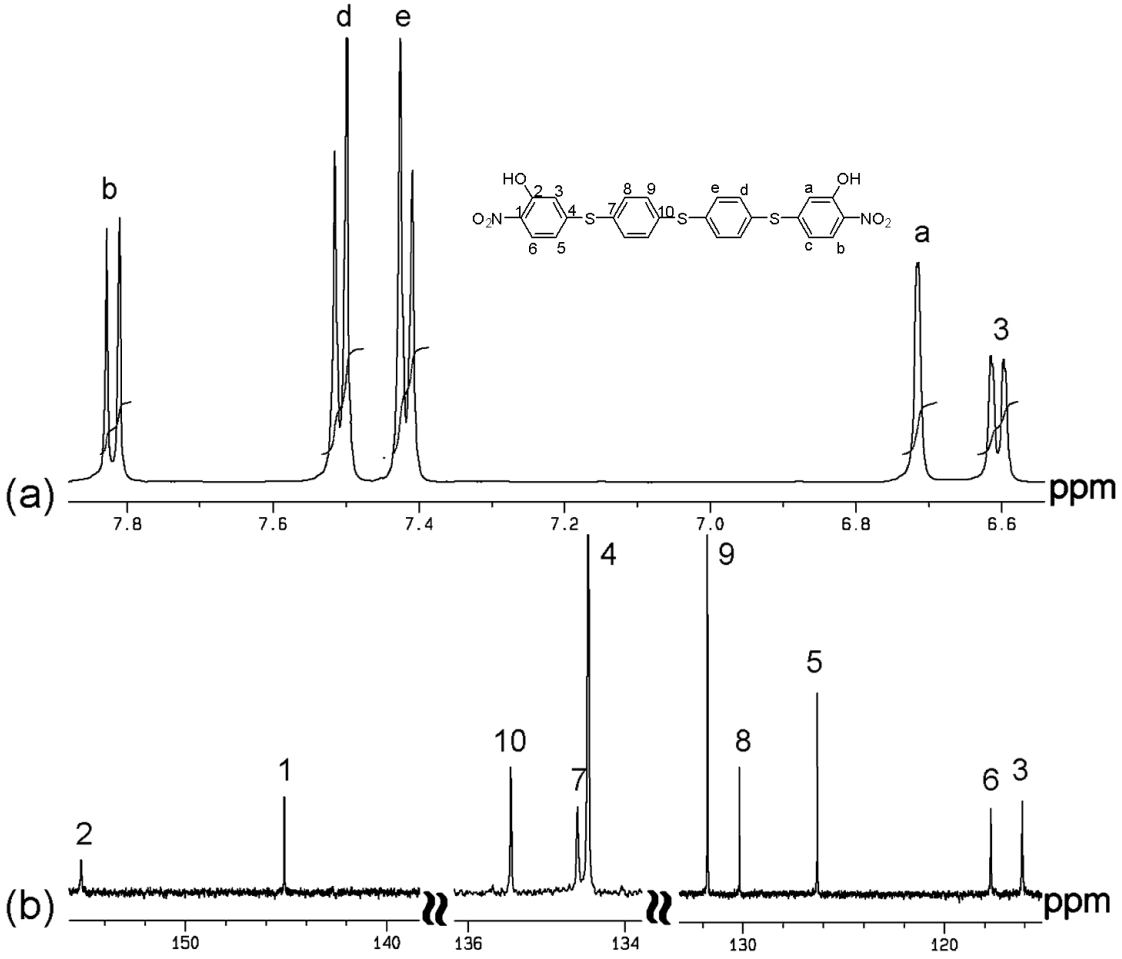

Figure S3. (a) ^{1}H NMR and **(b)** ^{13}C NMR spectra of compound **3S-DA** in DMSO-d_6.

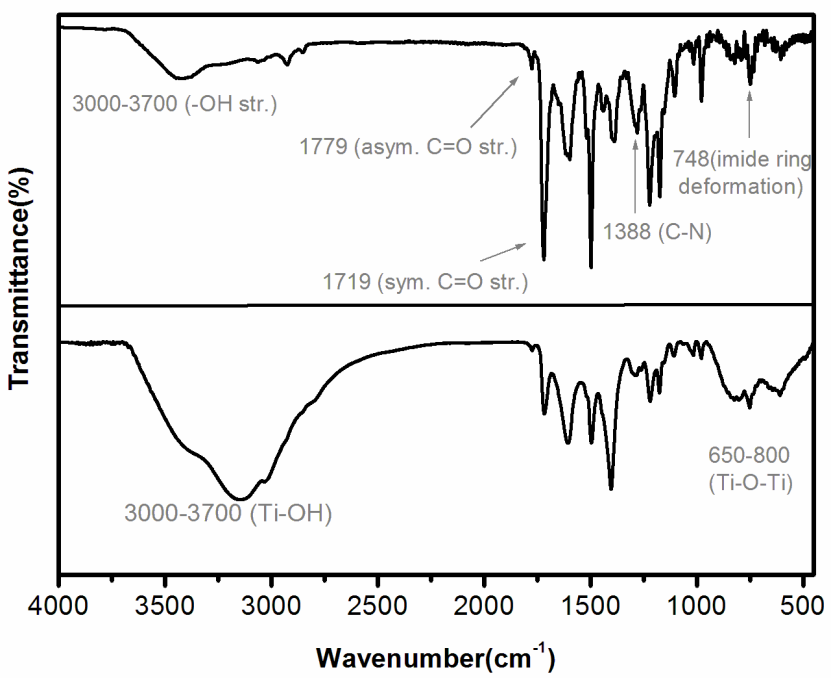

Figure S4. FT-IR spectra of the studied films (a) **F-PHI-b** and (b) **F-bTP50**.

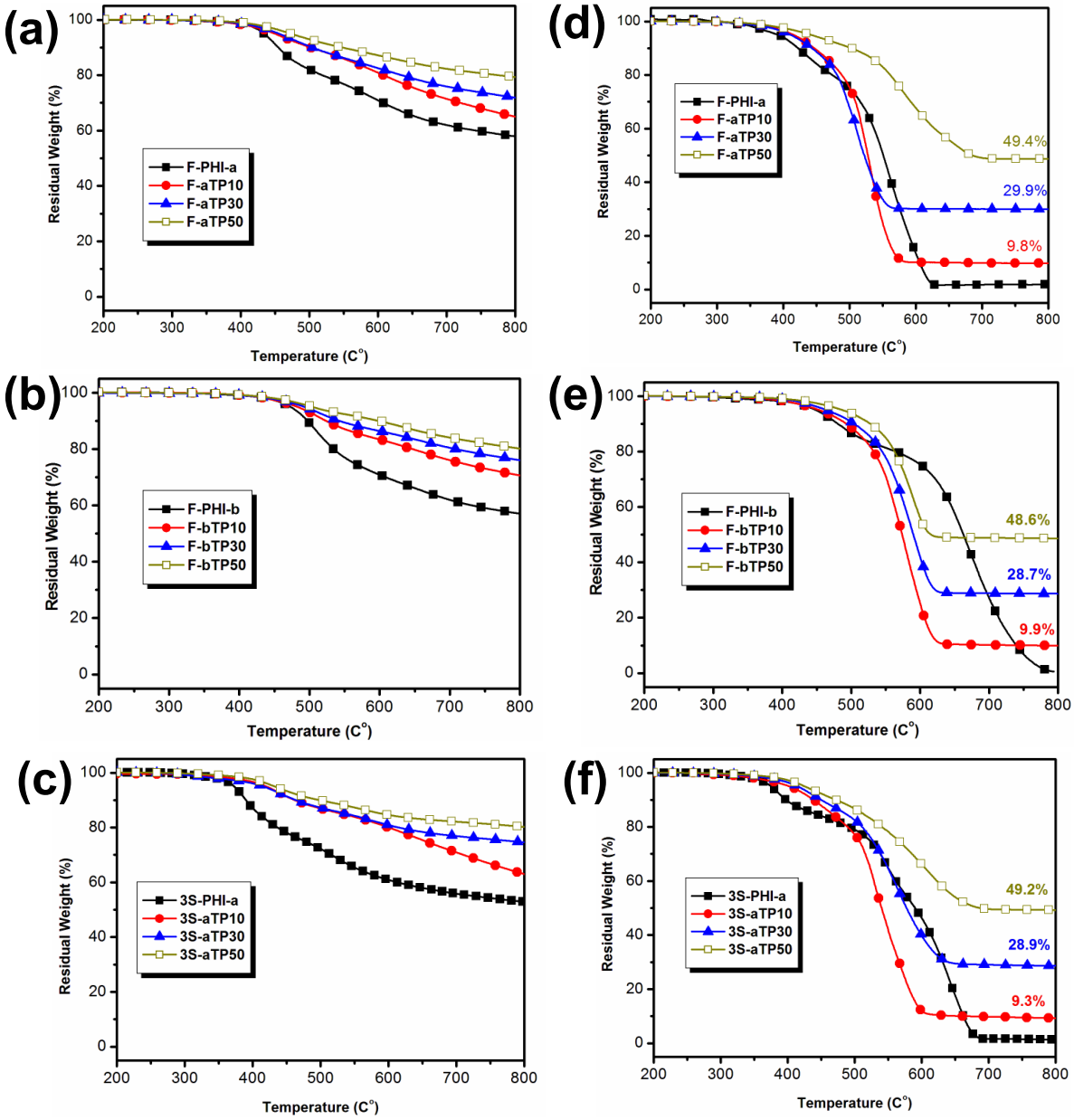

Figure S5. TGA thermograms of (a) **F-aTPX**, (b) **F-bTPX**, (c) **3S-aTPX** hybrid materials in nitrogen and (d) **F-aTPX**, (e) **F-bTPX**, (f) **3S-aTPX** hybrid materials in air.

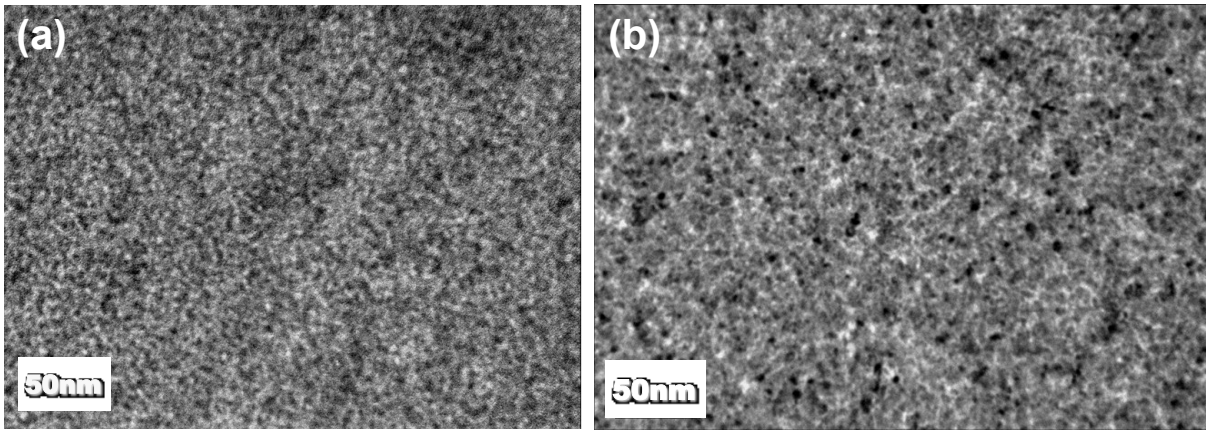

Figure S6. TEM image of the hybrid material (a) **F-aTP50** and (b) **3S-aTP50**.

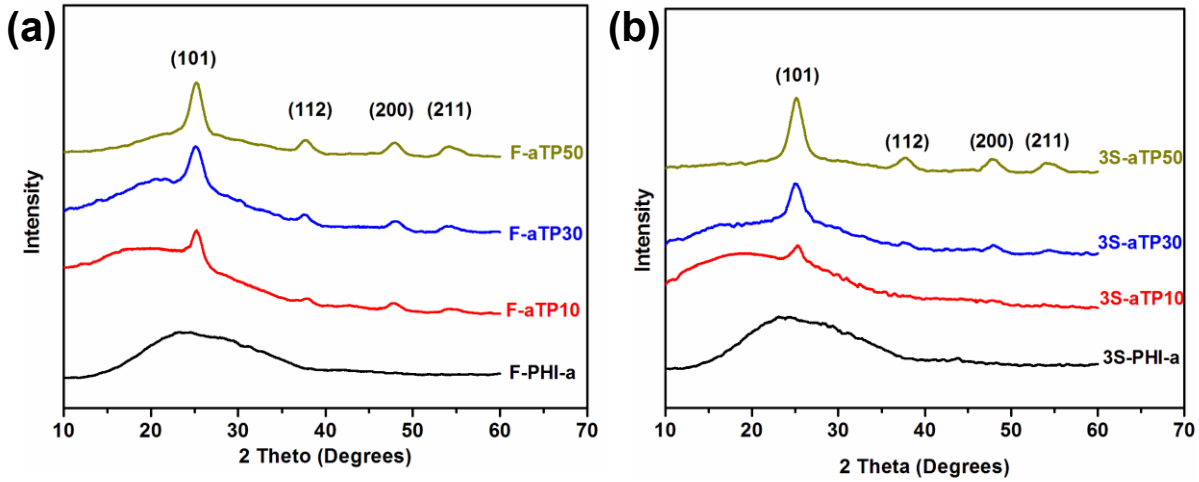

Figure S7. XRD patterns of (a) **F-aTPX** and (b) **3S-aTPX** hybrid materials.

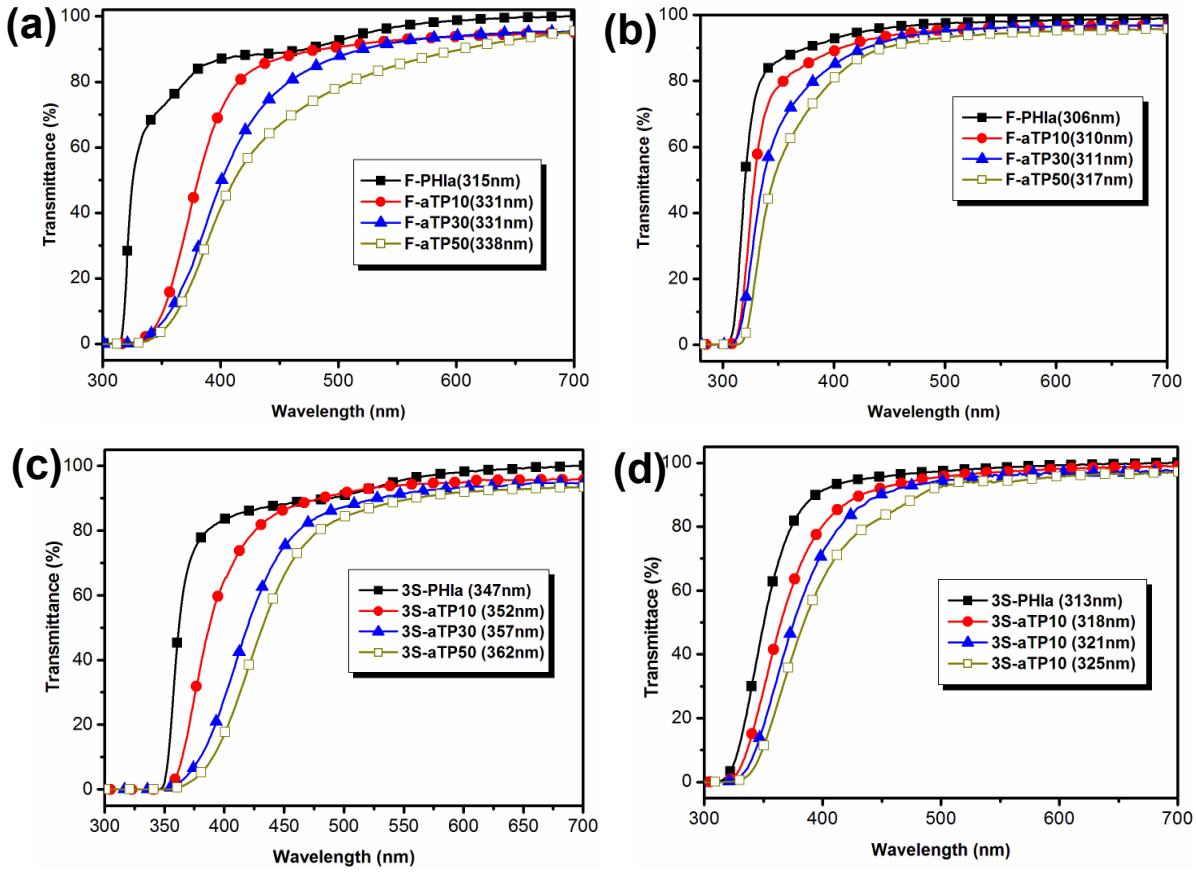

Figure S8. Transmittance UV-visible spectra of (a) **F-aTPX** thick films (13 ± 2 μm) (b) **F-aTPX** thin films (550~750nm), (c) **3S-aTPX** thick films (13 ± 2 μm), and (d) **3S-aTPX** thin films (550~750nm).

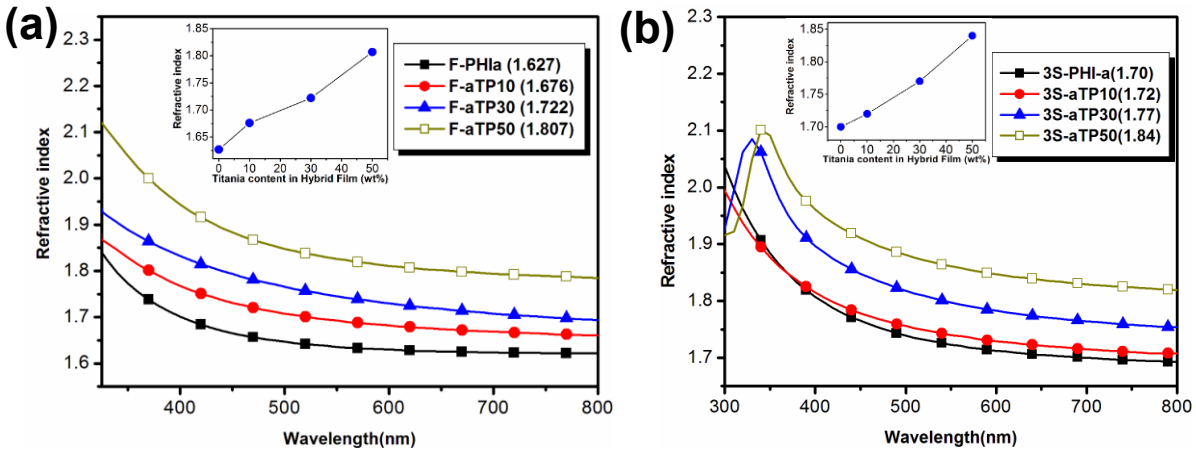

Figure S9. Variation of the refractive index of (a) **F-aTPX** and (b) **3S-aTPX** hybrid materials with wavelength. The insert figure shows the variation of refractive index at 633 nm with titania content.

Table S1. Reaction composition and properties of the **F-PHI-a** hybrid films

Polymer	Reactant compostition (wt%)		Hybrid film TiO_2 content (wt%)		
	F-PHI-a	$Ti(OBu)_4$	Theoretical	Experimental[a]	n^b
F-PHI-a	100	0	0	0	1.62
F-aTP10	67.8	32.2	10	9.8	1.67
F-aTP30	35.4	64.6	30	29.9	1.72
F-aTP50	19.0	81.0	50	49.4	1.80

[a] Experimental titania content estimated from TGA curves.

[b] *n*: Refractive index at 633nm by ellipsometer.

Table S2. Reaction composition and properties of the **3S-PHI-a** hybrid films

Polymer	Reactant compostition (wt%)		Hybrid film TiO_2 content (wt%)		
	3S-PHI-a	$Ti(OBu)_4$	Theoretical	Experimental[a]	n^b
3S-PHI-a	100	0	0	0	1.70
3S-aTP10	67.8	32.2	10	9.3	1.72
3S-aTP30	35.4	64.6	30	28.9	1.77
3S-aTP50	19.0	81.0	50	49.2	1.84

[a] Experimental titania content estimated from TGA curves.

[b] *n*: Refractive index at 633nm by ellipsometer.

Table S3. Thermal and Optical Properties of **F-PHI-a** Hybrid films

Index	Thermal Properties							Optical Properties		
	T_g (°C)[a]	CTE (ppm/K)[b]	T_d^5 (°C)[c]		T_d^{10} (°C)[c]		R_{w800} (%)[d]	λ_0 (nm)[e]	n[f]	Δn[g]
			N_2	Air	N_2	Air				
F-PHI-a	375	90	420	390	455	425	58	315	1.627	0.0073
F-aTP10	410	69	455	410	505	440	66	331	1.676	0.0088
F-aTP 30	417	57	455	410	505	445	72	331	1.722	0.0101
F-aTP 50	429	48	475	440	545	505	80	338	1.807	0.0132

[a] Glass transition temperature measured by TMA with a constant applied load of 10 mN at a heating rate of 10 °C min^{-1} by Tension mode.

[b] The CTE data was determined over a 50–200 °C range by expansion mode.

[c] Temperature at which 5% and 10% weight loss occurred, respectively, recorded by TGA at a heating rate of 20 °C/min and a gas flow rate of 30 cm^3/min.

[d] Residual weight percentages at 800 °C under nitrogen flow.

[e] The cutoff wavelength (λ_0) from the UV-vis transmission spectra of polymer films (thickness ~15μm).

[f] Refractive index at 633 nm by ellipsometer.

[g] The in-plane/out-of-plane birefringence (Δn) was calculated as $\Delta n = n_{TE} - n_{TM}$ were measured using a prism coupler.

Table S4. Thermal and Optical Properties of **3S-PHI-a** Hybrid films

Index	Thermal Properties							Optical Properties		
	T_g (°C)[a]	CTE (ppm/K)[b]	T_d^5 (°C)[c]		T_d^{10} (°C)[c]		R_{w800} (%)[d]	λ_0 (nm)[e]	n[f]	Δn[g]
			N_2	Air	N_2	Air				
3S-PHI-a	317	70	370	375	390	400	52	347	1.703	0.0173
3S-aTP10	361	64	420	400	460	440	63	352	1.725	0.0190
3S-aTP 30	373	55	420	415	465	450	74	357	1.776	0.0215
3S-aTP 50	385	42	430	425	500	470	79	362	1.844	0.0233

[a] Glass transition temperature measured by TMA with a constant applied load of 10 mN at a heating rate of 10 °C min^{-1} by Tension mode.

[b] The CTE data was determined over a 50–200 °C range by expansion mode.

[c] Temperature at which 5% and 10% weight loss occurred, respectively, recorded by TGA at a heating rate of 20 °C/min and a gas flow rate of 30 cm^3/min.

[d] Residual weight percentages at 800 °C under nitrogen flow.

[e] The cutoff wavelength (λ_0) from the UV-vis transmission spectra of polymer films (thickness ~15μm).

[f] Refractive index at 633 nm by ellipsometer.

[g] The in-plane/out-of-plane birefringence (Δn) was calculated as $\Delta n = n_{TE} - n_{TM}$ were measured using a prism coupler.